Shaping the Fluorescent Emission by Lattice Resonances in Plasmonic Crystals of Nanoantennas

G. Vecchi, V. Giannini, and J. Gómez Rivas*

Center for Nanophotonics, FOM Institute AMOLF, c/o Philips Research Laboratories,
High Tech Campus 4, 5656 AE Eindhoven, The Netherlands.
(Dated: March 13, 2009)

We demonstrate that the emission of light by fluorescent molecules in the proximity of periodic arrays of nanoantennas or plasmonic crystals can be strongly modified when the arrays are covered by a dielectric film. The coupling between localized surface plasmon resonances and photonic states leads to surface modes which increase the density of optical states and improve light extraction. Excited dye molecules preferentially decay radiatively into these modes, exhibiting an enhanced and directional emission.

Metallic nanoparticles are the object of a renewed scientific interest because of their remarkable optical properties, related to the excitation of localized surface plasmon resonances (LSPRs) [1, 2]. Advances in nanofabrication techniques allow to shape nanoparticles into the so-called optical antennas or nanoantennas. These techniques make possible to tune the LSPRs over a wide spectral range, providing control over the local field enhancement and far-field scattering [3]. Several studies have focused on the radiative properties of emitters in proximity to optical antennas [4–11]. The enhancement and quenching of the fluorescence by emitters close to metal nanoparticles have been described in terms of the balance between radiative and non-radiative decay rates [12–14]. These studies bring the twofold interest of, first, clarifying the fundamental processes of light-matter interaction at nanoscale and, second, the possible implementation of nanoantennas to enhance the efficiency of devices for lighting, photovoltaics, and sensing applications [15]. One limiting factor of metallic structures in general are their inherent losses [16]. Therefore, the prediction that the interaction between LSPRs of nanoparticles arranged in plasmonic crystals leads to mixed nanoparticle-lattice states or lattice surface modes in which the damping associated to individual particles is suppressed, can have implications in future nanoplasmonic research [17, 18]. These predictions have been confirmed in 1D and 2D plasmonic crystals [19–22] by the observation of sharp resonances in dark-field scattering and extinction spectra. Also the coupling between nanoparticles in 2D crystals through guided optical modes has been recently reported [23, 24]. However, the important question of how light emitters can couple to lattice surface modes and how their emission is influenced by this coupling still remains unexplored.

In this article, we demonstrate a strong modification and directional enhancement of the fluorescence of emitters in the proximity of plasmonic crystals of nanoantennas. This modified emission is the result of the electrodynamical coupling of the emitters to surfaces modes that result from the interaction of LSPRs with photonic states. We prove that the condition for the existence of these mixed modes, namely the embedding of the nanoparticle array in a fully symmetric dielectric environment, is less stringent than previously believed [21]. We support our conclusions with Finite-Difference-Time-Domain (FDTD) calculations.

Large arrays (3×3 mm^2) of gold nanoantennas were fabricated by nanoimprint onto a glass substrate with refractive index 1.52 at $\lambda = 700$ nm. A scanning electron microscope (SEM) image of the sample top is shown in the inset of Fig. 1(b). The height of the nanoantennas is 38 ± 2 nm. The grating constants are $a_x = 600 \pm 15$ nm and $a_y = 300 \pm 15$ nm. The nanoantennas are rectangular nanorods of rounded corners, with long (short) axis of 450 ± 10 nm (130 ± 10 nm) along the x (y) direction. An active layer of thickness 50 ± 10 nm, containing fluorescent molecules (ATTO 680) dispersed into a polyvinyl butyral (PVB) matrix with a concentration of 10^{-5} M, was spun onto the array. This top layer has a refractive index of 1.48 at $\lambda = 700$ nm.

Arrays of metallic nanoparticles may interact through coherent scattering processes. Diffractive coupling between LSPRs of the nanoparticles and photonic modes of the array occurs whenever the wavelength of the scattered light by LSPRs approaches the interparticle distance. The complex polarizability of an isolated particle, α, no longer describes such system. The array of nanoparticles, in the framework of the coupled dipole approximation, can be modeled by an effective polarizability $\alpha_{\mathrm{eff}} = \alpha/(1-\alpha S)$, where S is a term representing the retarded dipole sum resulting from coherent scattering in the nanoparticle array [18]. Scattering resonances, which give rise to lattice surface modes, arise whenever the real components of α^{-1} and S are equal [18, 25]. A reduction of the single particle damping also occurs because of the relative compensation of imaginary components of α^{-1} and S. This damping reduction produces sharp resonances [19–22]. As we show below, light emitters can couple very efficiently to these modes modifying their

emission characteristics and exhibiting narrow bands of enhanced emission.

A lattice resonance is displayed in Fig. 1(a) near to $\lambda = 900$ nm, where the red-solid line represents a measurement of the zero-order transmission at normal incidence through the plasmonic crystal on glass covered by the PVB layer. The measurement is normalized by the transmission through a substrate covered by a similar PVB layer. We illuminated the sample with a beam from an halogen lamp with the polarization parallel to the short axis of the nanoantennas. The broad reduction of the transmittance around 680 nm corresponds to the extinction resulting from the excitation of the half-wave LSPR in each individual nanoantenna. The asymmetric and narrower resonance around 900 nm arises from the diffractive coupling of the nanoantennas arranged in the plasmonic crystal. It has been highlighted the importance of surrounding the nanoparticles by a homogeneous dielectric environment in order to obtain an effective diffractive coupling [21]. Fig. 1(a) shows the transmittance measured through a similar array without top PVB layer (black-dotted line). The single particle LSPR is shifted to 620 nm due to the reduced permittivity of the surrounding medium. The major difference compared to the measurement of the sample with the PVB layer is the disappearance of the lattice surface mode, as a result of the inefficient diffractive coupling in the inhomogeneous environment. We stress that the nanoantenna array covered by PVB is not in a fully symmetric dielectric environment. Instead, there is a small difference in refractive index between the glass substrate and the polymer layer, and this layer has a finite thickness of 50 nm. Therefore, the condition for the existence of these modes, namely, an homogeneous dielectric environment around the nanoparticle array, is less stringent than believed.

The main features in the measurements of Fig. 1(a), i.e., the LSPR and the lattice resonance, are well reproduced by FDTD calculations in Figure 1(b). The shoulder around $\lambda = 600$ nm due to intraband transitions in gold is much less pronounced in the measurements. Calculations of the near field enhancement, i.e., the near field intensity normalized by the incident intensity, are shown in Fig. 2 for two different wavelengths, (a) 695 nm and (b) 905 nm. At $\lambda = 695$ nm, i.e., the wavelength of the LSPR, the field is enhanced at the edges of nanoantennas. On the contrary, the diffractive coupling of nanoantennas leading to the lattice surface mode at $\lambda = 905$ nm produces a drastic redistribution of the near field with a much larger enhancement in between the nanoantennas. This lattice surface mode represents a new decay channel for dye molecules in the proximity of the nanoantenna crystal.

To obtain the dispersion relation of these modes, we have measured the zero-order transmission spectra as a function of the incident angle θ_{in} in the range $0° - 50°$. These measurements are displayed in Fig. 3(a) as a function of $k_\parallel$, where $\mathbf{k}_\parallel = k_\parallel \hat{x} = k_0 \sin(\theta_{in})\hat{x}$, and $k_0 = \omega/c$. The so-called Rayleigh anomalies, or the

condition at which a diffracted order becomes grazing to the grating surface, have been also plotted in Fig. 3 with black lines. These anomalies are given by the equation $k_{out}^2 = k_{in}^2 \sin^2 \theta_{in} + m_1^2 (2\pi/a_x)^2 + m_2^2 (2\pi/a_y)^2 + 2k_{in} \sin \theta_{in} m_1 (2\pi/a_x)$, where k_{in} and k_{out} are the incident and scattered wave numbers, and (m_1, m_2) are integers defining the diffraction order. The Rayleigh anomalies displayed in Fig. 3 were calculated taking a refractive index $n = 1.50$, which corresponds to the average between the glass and PVB indices. The LSPR at $\omega/c = 0.0092$ rad nm^{-1} is manifest in Figs. 3(a) and (b) by the broad reduction in transmittance. The localized nature of this resonance, as it was apparent in Fig. 2 (a), is also evident from its flat dispersion. The surface modes resulting from the diffractive coupling of LSPRs appear as narrow bands of reduced transmittance at lower frequencies than the Rayleigh anomaly. Let us focus on the mode associated to the (1,0) diffraction order. As the frequency increases towards the LSPR frequency, the wave number of the surface mode deviates from the Rayleigh anomaly and also the width of the resonance increases [21]. The dispersive behavior of these modes is similar to that of surface plasmon polaritons propagating on metallic gratings.

In the following, we focus on the emission of the dye molecules embedded in the PVB layer and their coupling to the lattice surface modes. The one photon fluorescence enhancement of an emitter excited below saturation is defined as the emitted intensity (I) normalized by the intensity of the emitter in the absence of the plasmonic crystal (I_0). For randomly oriented dipoles, this enhancement is given by

$$\frac{I}{I_0} = \frac{\eta(\mathbf{r}_0, \omega_{em})}{\eta_0(\mathbf{r}_0, \omega_{em})} \frac{|\mathbf{E}(\mathbf{r}_0, \omega_{abs})|^2}{|\mathbf{E}_0(\mathbf{r}_0, \omega_{abs})|^2} , \qquad (1)$$

where $\mathbf{E}$ and $\mathbf{E}_0$ are the local and incident electric fields at the pump frequency ω_{abs} and η and η_0 are the quantum yield of molecules with and without the presence of the nanoantennas. The term $|\mathbf{E}|^2/|\mathbf{E}_0|^2$ represents the pump enhancement, or the increase of fluorescence of an emitter located at $\mathbf{r}_0$ due to the local enhancement of the field at the frequency of excitation. The term η/η_0 corresponds to the increase of emission due the enhancement of the local density of optical states (LDOS) at $\mathbf{r}_0$ to which the emitter can decay emitting radiation of frequency ω_{em}.

To investigate the emission of sources coupled to plasmonic crystals, we have performed fluorescence measurements of ATTO 680 molecules embedded in the PVB layer. ATTO 680 is a photostable dye with a maximum absorption cross section at $\lambda = 680$ nm and a fluorescence spectrum peaked at 700 nm and extending until 950 nm. The dye molecules were excited at a fixed angle of illumination ($\theta_{in} = 50°$) using a laser diode at $\lambda = 685$ nm. At this wavelength ATTO 680 absorbs very efficiently and the unfocused pump, of beam size ~ 1 mm, excites uniformly the molecules over a large area. The laser power, 1 mW, was weak enough to neglect saturation effects. We detected the fluorescence emission with

polarization parallel to the short axis of the nanoantennas. The angular detection range of the fluorescence was from 0° to 40° in the plane of incidence. The measurements are displayed in Figure 4. Figure 4(a) represents the fluorescence intensity measured on the array normalized to the fluorescence of a similar layer of PVB and dye molecules on top of an unpatterned substrate. The normalized fluorescence is represented as a function of $k_{\parallel}$ and of the normalized frequency ω/c. For a direct comparison with the variable-angle transmittance measurements, we display these measurements in Fig. 4(b) in the same range of wave numbers and frequencies than the fluorescence measurements. In Fig. 4(c) we display three normalized fluorescence spectra obtained from Fig. 4(a) at different values of $k_{\parallel}$. It is evident from Figs. 4(a) and (b) that the highest enhancement of the fluorescence (up to seven-fold enhancement) takes place on a narrow band that follows the dispersive behavior of the lattice surface mode resulting from the diffractive coupling of LSPRs.

To rule out a possible contribution of a local pump enhancement to the fluorescence emission, we have measured the transmittance spectrum (Fig. 5(a)) through the plasmonic crystal for an incident angle $\theta_{\mathrm{in}} = 50°$, i.e., the angle of incidence of the pump laser. The polarization of the light was set parallel to the long axis of the nanorods, as was for the excitation beam during the fluorescence measurements. The reductions of the transmittance around 900 nm and 650 nm in Fig. 5(a) are due to the excitation of the second and third order LSPRs along the long axis of the nanoantennas. The most relevant feature in Fig. 5(a) for our measurements is the high transmittance at $\lambda = 685$ nm, which indicates the absence of resonant scattering by the nanoantennas at the wavelength of the pumping laser. This absence of resonant scattering leads to a negligible local field enhancement as can be appreciated in the FDTD calculation of Fig. 5(b).

Being discarded the contribution of a local field enhancement of the pump to the fluorescence, the large directional enhancement of the emission in Fig 4 is attributed to the first factor of Eq. (1), i.e., to an increase of the LDOS associated to lattice surface modes to which the excited dye molecules can decay radiatively. The de-

localized nature of these modes, with a large field intensity distributed in between the nanoantennas, is advantageous over the LSPRs for an efficient emission because of the following reasons: (i) a larger number of dye molecules can efficiently couple to this mode due to its large extension; (ii) The average distance between fluorescent molecules that couple to the mode and the metal is larger, which reduces the metal induced fluorescence quenching, and (iii) the dispersion relation of surface mode is close to the Rayleigh anomaly (black line in Fig. 4(a)), which means that a small extra momentum is required to efficiently couple out the fluorescence to radiative modes. This last point is clearly visible in Figs. 4(a) and (c), where the fluorescence enhancement at the lattice resonance gradually decreases for increasing $k_{\parallel}$ or as the resonance deviates from the Rayleigh anomaly. It is important to notice that only a weak enhancement of the emission is observed at the LSPR, i.e., at $\lambda = 700$ nm, which highlights the higher efficiency of lattice surface modes over LSPRs for light extraction in the proximity of plasmonic crystals. A similar enhancement was observed around 900 nm for the emission polarized parallel to the long axis of the nanoantennas, most likely due to the second order LSPR.

In summary, we have demonstrated that lattice surface modes resulting from the coupling of localized surface plasmon resonances in plasmonic crystals of nanoantennas are responsible of a strong modification of the emission properties of dye molecules in proximity of the crystal. Enhanced fluorescence, due to the increased local density of optical states to which dye molecules can decay, has been measured within narrow spectral and angular bands. This observation introduces new perspectives in the field of surface enhanced fluorescence for, e.g., microscopy imaging, biology, and optical devices.

[1] S. A. Maier and H. A. Atwater, J. Appl. Phys. **98**, 011101 (2005), and references therein.
[2] S. Lal, S. Link, and N. J. Halas, Nature Photonics **1**, 641 (2007), and references therein.
[3] P. Mühlschlegel *et al.*, Science **308**, 1607 (2005).
[4] J. R. Lakowicz, Anal. Biochem. **337**, 171 (2005).
[5] S. Kühn *et al.*, Phys. Rev. Lett. **97**, 017402 (2006).
[6] H. Mertens *et al.*, Nano Lett. **6**, 2622 (2006).
[7] S. Gerber *et al.*, Phys. Rev. B **75**, 073404 (2007).
[8] F. Tam *et al.*, Nano Lett. **7**, 496 (2007).
[9] O. Muskens *et al.* Nano Lett. **7**, 2871 (2007).
[10] R. M. Bakker *et al.*, Appl. Phys. Lett. **92**, 043101 (2008).
[11] M. Ringler *et al.*, Phys. Rev. Lett. **100**, 203002 (2008).
[12] G. W. Ford and W. H. Weber, Phys. Rep. **113**, 195 (1984).
[13] E. Dulkeith *et al.*, Nano Lett. **5**, 585 (2005).
[14] P. Anger, P. Bharadwaj, and L. Novotny, Phys. Rev. Lett. **96**, 113002 (2006).
[15] A. Polman, Science **322**, 868 (2008).
[16] J. B. Khurgin, G. Sun, and R. A. Soref, J. Opt. Soc. Am. B **24**, 1968 (2007).
[17] K. T. Carron *et al.*, J. Opt. Soc. Am. B **3**, 430 (1986).
[18] S. Zou, N. Janel, and G. C. Schatz, J. Chem. Phys. **120**, 10871 (2004).

[19] E. M. Hicks *et al.*, Nano Lett. **5**, 1065 (2005).

[20] V. G. Kravets, F. Schedin, and A. N. Grigorenko, Phys. Rev. Lett. **101**, 087403 (2008).

[21] B. Auguié and W. L. Barnes, Phys. Rev. Lett. **101**, 143902 (2008).

[22] Y. Chu *et al.*, Appl. Phys. Lett. **93**, 181108 (2008).

[23] S. Linden, J. Kuhl, and H. Giessen, Phys. Rev. Lett. **86**, 4688 (2001).

[24] N. Félidj *et al.*, Phys. Rev. B **66**, 245407 (2002).

[25] F. J. García de Abajo *et al.*, Opt. Express **14**, 7 (2006).
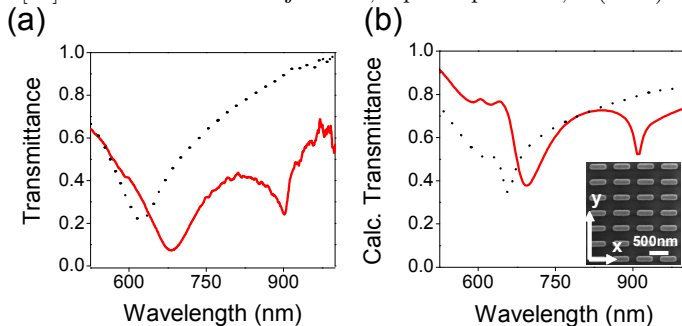
FIG. 1: (a) Measurements and (b) FDTD calculations of the transmittance through a 2D plasmonic crystal of gold nanoantennas on top of a glass substrate (black-dotted lines) and through a similar plasmonic crystal covered by a 50 nm thick PVB layer (red-solid lines). Inset in (b): SEM image of a plasmonic crystal.
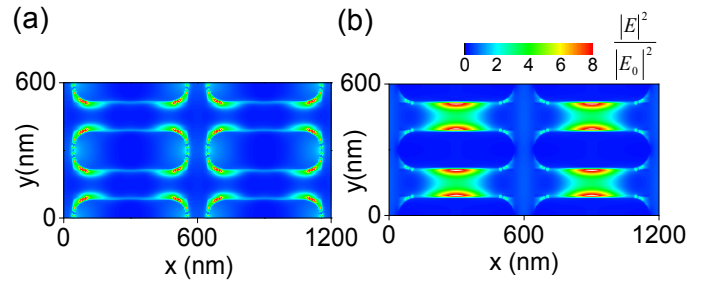

FIG. 2: Near field intensity enhancement in a 2D plasmonic crystal of nanoantennas on a glass substrate covered by a PVB layer. The field is calculated on the plane intersecting the nanoantennas at their middle height (z = 20 nm). The calculations are at (a) $\lambda = 695$ nm, and (b) $\lambda = 905$ nm, which correspond to the LSPR and to the lattice surface mode respectively.
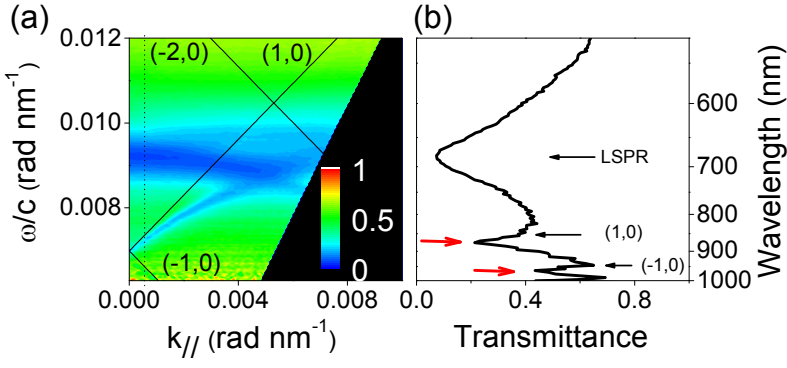
FIG. 3: (a) Transmittance of light polarized parallel to the short axis of the nanoantennas as a function of the normalized frequency, ω/c, and the wave number $k_\parallel$. The solid lines represent the Rayleigh anomalies. (b) Transmittance spectrum at $k_\parallel = 5.47 \times 10^{-4}$ rad nm^{-1}, i.e., the wave vector indicated by the dotted vertical line in (a). Thin black arrows indicate the Rayleigh condition and the LSPR, the thick red arrows indicate the lattice surface resonances.
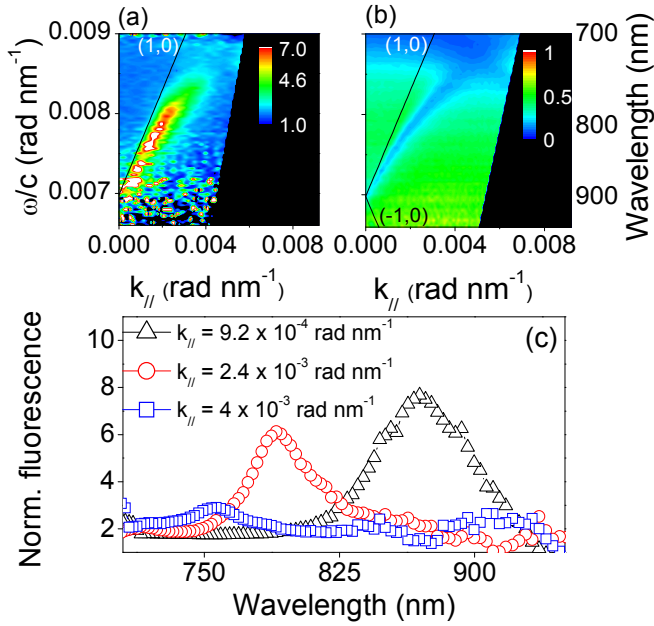

FIG. 4: (a) Fluorescence enhancement or the fluorescence of dye molecules in the proximity of a plasmonic crystal normalized by the fluorescence of dye molecules on an unpatterned substrate. (b) Transmittance as in Fig. 3(a). (c) Fluorescence enhancement spectra at three different values of $k_\parallel$.
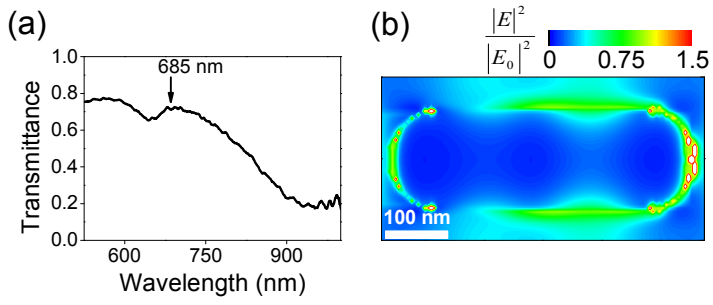
FIG. 5: (a) Transmittance spectrum through a plasmonic crystal of nanoantennas for incident angle $\theta_{in} = 50°$ and polarization parallel to the long axis of nanoantennas. (b) FDTD calculation of the near field intensity enhancement around one nanoantenna at a wavelength of 685 nm and for an angle of incidence $\theta_{in} = 50°$.